Desalination and Water Treatment
www.deswater.com

doi: 10.5004/dwt.2022.28483

259 (2022) 186–196
May

A mathematical model for simulation the removal of cadmium and chromium from groundwater using scrap iron and aluminum as permeable reactive barrier

Ayad A.H. Faisal[a], Hayder M. Rashid[b], Gaurav Sharma[c,d,e], Nadhir Al-Ansari[f,*], B. Saleh[g]

[a]*Department of Environmental Engineering, College of Engineering, University of Baghdad, Baghdad, Iraq, Tel. +9647904208688; email: ayadabedalhamzafaisal@yahoo.com*
[b]*Department of Environmental Engineering, College of Engineering, University of Baghdad, Baghdad, Iraq, email: h.m.rasheed@coeng.uobaghdad.edu.iq*
[c]*College of Materials Science and Engineering, Shenzhen Key Laboratory of Polymer Science and Technology, Guangdong Research Center for Interfacial Engineering of Functional Materials, Nanshan District Key Lab. for Biopolymers and Safety Evaluation, Shenzhen University, Shenzhen 518055, P.R. China, email: gaurav8777@gmail.com*
[d]*International Research Centre of Nanotechnology for Himalayan Sustainability (IRCNHS), Shoolini University, Solan 173212, Himachal Pradesh, India*
[e]*School of Life and Allied Health Sciences, Glocal University, Saharanpur, India*
[f]*Department of Civil, Environmental and Natural Resources Engineering, Lulea University of Technology, 97187 Lulea, Sweden, email: nadhir.alansari@ltu.se*
[g]*Mechanical Engineering Department, College of Engineering, Taif University, P.O. Box: 11099, Taif 21944, Saudi Arabia, email: b.saleh@tu.edu.sa*

Received 10 August 2021; Accepted 4 April 2022

ABSTRACT

The present work is represented by the derivation of mathematical model and solving the model analytically using the method of separation of variables to describe the migration of the contaminant metal ions through a column packed with bed of permeable reactive barrier (PRB). The validity of the solution can be evaluated through the simulation of cadmium and chromium ions using scrap iron and/or aluminum by-products in the form of wastes that if not utilized to treat waste by waste can impose further burden over the ecosystem. Breakthrough curves proved that the increase of metal ions velocity will decrease the capturing of the ions; therefore, the distribution coefficient and the retardation factor also decrease. Furthermore, the increase of barrier depth will increase the longevity of PRB because this will delay the migration of contaminant. A mathematical model has acceptable ability in the representation of experimental measurements with Nash–Sutcliff efficiency coefficients greater than 0.98. The longevity of the PRB was estimated for the field scale to be 210 and 250 d to produce contaminant effluent beyond 100 cm barrier matrix within the environmental permissible concentrations. Although groundwater velocity is highly variable, a proposed velocity of 0.25 cm/min which is assumed to be analogous to the groundwater velocity has revealed prolonged longevity of 7.02 y for the capture of chromium.

Keywords: Modeling; Zero-valent iron; Zero-valent aluminum; Groundwater contamination; Solute transport

* Corresponding author.

1. Introduction

The widespread contamination of surface water and groundwater with heavy metals has created serious problems for the ecosystem. Due to the complex co-existence, mobile nature, toxicity, high relative density; these metals infiltrate into the soil and pollute the surface and groundwater systems. Rather than the anthropogenic sources, the natural sources of pollution also contribute largely to the contamination of these vital water bodies [1–3]. For example, the prolonged presence of cadmium and chromium metals will endanger aquatic livings and mankind even at low concentrations [4,5]. Many regulations specified the permissible concentrations for cadmium (Cd(II)) and chromium (Cr(III)) to be 0.005 and 0.1 mg/L respectively [6]. Although trivalent chromium is an essential microelement for humans and is nontoxic in normal doses in the food supply; at higher doses, however, it can exhibit cytotoxicity. Also, despite chromium(III) is much less toxic than chromium(VI), the respiratory tract is also the major target organ for chromium(III) toxicity similar to chromium(VI).

The ongoing deterioration of the ecosystem has rendered the urgent need for particular remediation techniques to get rid of all these pollutants. The "impermeable barriers" and "pump and treat" systems are examples of the most conventional remedial techniques used so far; but the high costs, as well as difficulties concomitant with the operation and maintenance, would render these passive in situ remediation techniques unfavorable [7,8]. In this direction, the permeable reactive barrier (PRB) has proven to be one of the most practical approaches in treating heavy metals. These barriers capture the pollutants that permeate through the saturated zone and therefore enhance the natural attenuation processes occurring in soil. The mobility of heavy metals dissolved in groundwater might be controlled by reactions that cause metals to be adsorbed or to precipitate [9].

Prior to this study, several studies have been examined such as the sorption of copper and chromium on lateritic silty-clay soils [10], the batch study using zero-valent iron as a reactive medium for the removal of high-level arsenite from groundwater [11], the biosorption of Cr(III) onto *Agave lechuguilla* biomass [12]. Deep discussion for removal efficiencies and reaction mechanisms due to interaction of zero-valent iron with inorganic and organic chemicals were introduced [13]. The effect of inexpensive and available zero-valent iron on the removal of zinc ions from the contaminated groundwater was implemented. The study was furnished with a mathematical model that can be solved using computer techniques with the aid of COMSOL software [14]. The optimum conditions for clarifying wastewater from the dissolved heavy metals using an acid prewashed zero-valent iron (ZVI) and/or zero-valent aluminum (ZVAI) as PRB were studied [15]. Many extensive studies were directed to study the ability of PRB in the remediation of aqueous solutions contaminated with different types of heavy metals using different materials like zeolite [16], waste foundry sand [17], cement kiln dust [18], sewage sludge [19], waterworks sludge [20], iron slag [3], coated sand by iron oxide [21], and activated carbon – waste foundry sand composite sorbent [22].

Huge amounts of scrap iron and alumina were produced every day in industrial workshops distributed in Baghdad, Iraq with average daily rates reached up to 13.2 and 0.24 tons per capita respectively. These scrap wastes are banished to the ecosystem, so, their reuse as reactive materials in the PRBs for the elimination of heavy metals from contaminated groundwater can be considered as an application in the field of sustainable development. The uniqueness of this investigation is achieved the continuous study supported by the derivation of a mathematical model with an analytical solution to present a conceptual vision for the migration of cadmium and/or chromium ions in the one-dimensional ZVAI and/or ZVI packed bed columns respectively. Hence, the main aims are; (i) investigating the possibility of using ZVI/ZVAI as inexpensive by-product materials in the PRB for capturing cadmium and/or chromium ions, (ii) treating waste by another waste to reduce remediation costs to a minimum (iii) developing a mathematical model solved analytically to characterize the one-dimensional contaminant transport.

2. Experimental work

2.1. Preparation of ZVI/ZVAI

The ZVI (Fig. 1a) was prepared as follows [11]; (1) purifying the raw scrap iron at which iron was magnetically separated from other impurities (grit, dirt, hairs, and stubs), (2) sieving the purified iron using a sieve with mesh number (75) to produce uniform iron solid particles of 1.5 mm, and (3) chemically prewashing the purified iron in such a way the ZVI is immersed in 0.1 M H_2SO_4 solution for 10 min and then in acetone for 30 min and finally rinsed in distilled water three times.

The ZVAI (Fig. 1b) was prepared as follows [11]; (1) purifying the raw scrap alumina by sorting out splinters, screws, and other foreign substances, (2) soaking the purified scrap alumina as it is in benzene for 10 min to remove grease and oils, and(3) chemically prewashing the purified and degreased alumina, the ZVAI (with particles diameter identical to that of ZVI) is slowly added to (10 mL) concentrated HCI, a 0.5 mL of 0.5 M H_2SO_4 was added to dissipate heat generated and the suspension was stirred for 20 min and filtered.

2.2. Contaminants

A 50 mg/L of both Cd(II) and Cr(III) concentrations were prepared by dissolving certain quantities of cadmium nitrate (2.1032 g $Cd(NO_3)_2$) or hydrated chromium nitrate (7.696 g $Cr(NO_3)_3{\cdot}9H_2O$) in 250 mL of deionized water for the preparation of cadmium and/or chromium stock solution respectively. The solution was diluted to 1 L in a volumetric flask and stored in a polythene bottle where the concentration of metal can be measured in the emission at 326.1 nm for cadmium and 425.4 nm for chromium using air-acetylene flame atomic absorption spectrophotometer (AAS) type Shimadzu, 635 D, Japan and according to the conventional Standard Methods. The AAS device was calibrated using operational standard solutions covering the expected concentration range of the samples.

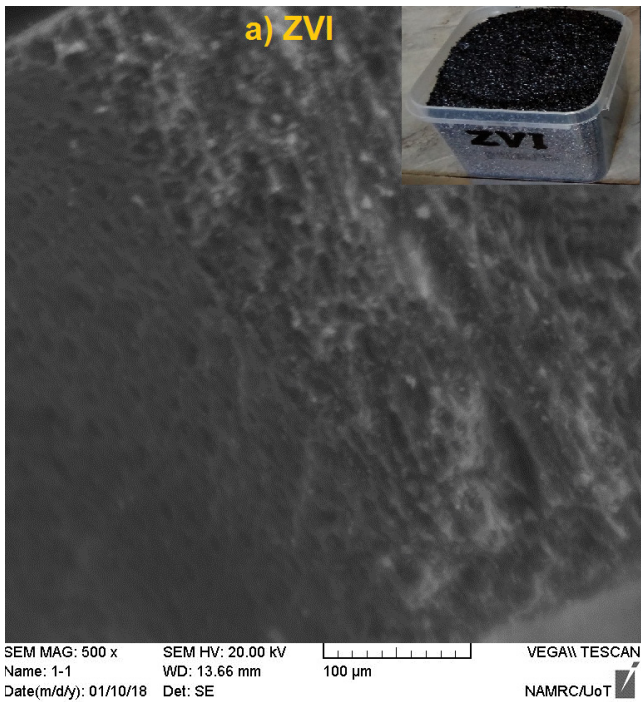

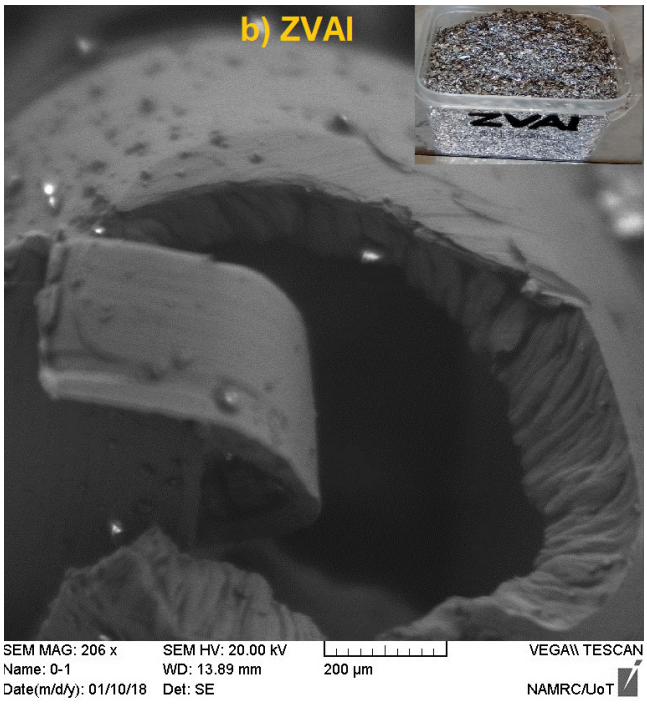

Fig. 1. Appearance of (a) ZVI and (b) ZVAI sorbents with their surface morphologies imaged by SEM analysis.

2.3. Column tests

Five columns of Pyrex glass were installed; each column (125 cm length and 1.6 cm inner diameter) was packed with a specified depth of reactive materials. This means that columns 1, 2, 3, 4, and 5 were packed with depths of 20, 40, 60, 80, and 100 cm respectively as illustrated in Fig. 2a. These columns are equipped with several ports for sampling depended on the depth of the reactive bed. An infusion set (Fig. 2b) was connected to each port for easily controlling the withdrawal of aqueous solution samples for concentration measurements. The infusion sets are more secure and accurate than syringes to withdraw 1 mL of water sample without probable disruption of the flow in the porous medium for the packed bed. The ports are equally spaced at which any two adjacent ports are 20 cm apart, except the first port is located at the base of the bed.

The packs of the columns are composed of ZVI, ZVAI, or a mixture of these two materials. This mixture consisted of 86% ZVI and 14% ZVAI (i.e., 6 g ZVI/1 g ZVAI). Distilled water was pumped through the columns at a low rate to expel air entrapped within the bed voids. The simulated contaminated groundwater in the source tank was adequately fed from the bottom of the columns by using a peristaltic pump at different volumetric flow rates of 3, 4.5, 6, and 7.5 mL/min with corresponding apparent velocities of 1.50, 2.25, 3.00, and 3.75 cm/min. Frequent observations have been triggered along with the columns and water samples were withdrawn from each port every almost 2 h then up to 24 and 48 h to track down the contaminant propagation through the packed bed.

3. Mathematical model

Solutions of the governing equations may yield exact predictions in the form of analytical solutions that satisfy minimal error between the experimental values and the theoretical outputs of hydro-physical parameters such as head, potential, flux, concentration, and others. Most complex groundwater systems can hardly be tackled with analytical solution approaches and the omission or approximation of some parameters in the governing equation may produce a satisfactory solution with the acceptable magnitude of error [23]. The partial differential advection-dispersion equation for one-dimensional contaminant propagation in porous media can be written as follows:

$$R\frac{\partial C}{\partial t} = D\frac{\partial^2 C}{\partial z^2} - U\frac{\partial C}{\partial z} \tag{1}$$

where R is the retardation factor (dimensionless), D is the dispersion coefficient (cm^2/min), and U is the seepage water velocity (cm/min). The governed equation with the given boundary and initial conditions; $C(0,t) = C_o$ mg/L, $\partial C / \partial z = 0$ at $z=H$; $C(z,0) = 0$ mg/L can analytically be solved using Fourier transform, Laplace transform, or separation of variables. The mathematical model is used in predicting the contaminant breakthrough curves making use of the separation of variables method that can be outlined as follows [24,25]:

The non-homogeneous boundary conditions render the solution by the method of separation of variables harder; therefore, they must be transformed into homogenous ones by letting:

$$C(z,t) = \Phi(z,t) + f(z) \tag{2}$$

Substituting into Eq. (1) yields:

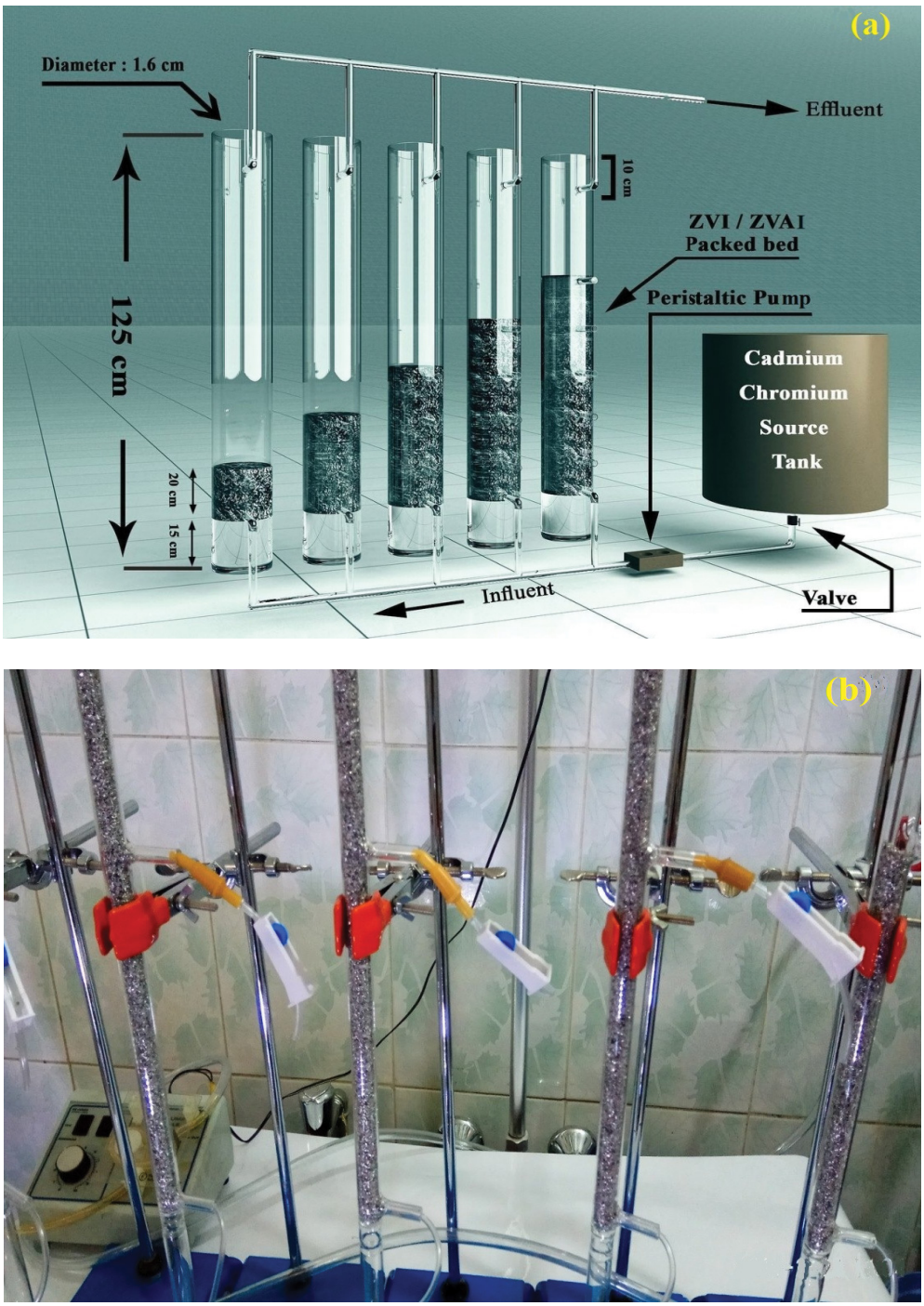

Fig. 2. (a) A schematic diagram for the columns configuration and (b) photo image for the columns configuration.

$$R\frac{\partial \Phi}{\partial t} = D\left(\frac{\partial^2 \Phi}{\partial z^2} + \frac{d^2 f}{dz^2}\right) - U\left(\frac{\partial \Phi}{\partial z} + \frac{df}{dz}\right) \tag{3}$$

Now, Eq. (3) is a combination of Eqs. (4) and (5):

$$R\frac{\partial \Phi}{\partial t} = D\left(\frac{\partial^2 \Phi}{\partial z^2}\right) - U\left(\frac{\partial \Phi}{\partial z}\right) \tag{4}$$

$$D\left(\frac{d^2 f}{dz^2}\right) - U\left(\frac{df}{dz}\right) = 0 \tag{5}$$

The second-order ordinary differential Eq. (5) has the following solution:

$$f(z) = ae^{U_z/D} + b \tag{6}$$

The arbitrary constants a and b can be determined via substituting the boundary conditions such that:

The $C(0,t) = \Phi(0,t) + f(0) = C_o$ and if $\Phi(0,t) = 0$, then $f(0) = C_o$, that is,

$$a + b = C_o \tag{7}$$

$$\frac{\partial C(z,t)}{\partial z} = \frac{\partial \Phi(z,t)}{\partial z} + \frac{df(z)}{dz} \text{ or}$$
$$\frac{\partial C(H,t)}{\partial z} = \frac{\partial \Phi(H,t)}{\partial z} + \frac{df(H)}{dz} = 0 \tag{8}$$

If $\frac{\partial \Phi(H,t)}{\partial z} = 0$, then $\frac{df(H)}{dz} = 0$ (i.e., $a\frac{U}{D}e^{UH/D} = 0$

Neither velocity nor the exponential terms are equal to zero; therefore, substituting $a = 0$ into Eq. (7), yields $b = C_o$, however, substituting a and b reduces Eq. (6) into $f(z) = C_o$, and since $C(z,0) = \Phi(z,0) + f(z) = 0$; the new initial condition will be:

$$\Phi(z,0) = -C_o \tag{9}$$

The non-homogeneous boundary conditions are transformed into homogeneous ones and separating variables can easily be applied by letting:

$$\Phi = ZT \tag{10}$$

where $Z = Z(z)$ and $T = T(t)$, substituting into Eq. (5) yields:

$$R\frac{\partial T/\partial t}{T} = D\frac{\partial^2 Z/\partial z^2}{Z} - U\frac{\partial Z/\partial z}{Z} = k \tag{11}$$

The proportionality constant (k) may take positive, zero, or negative values (i.e., μ^2, 0, $-\mu^2$). The first two possible values yield a trivial solution while the latter value yields a non-trivial one and consequently:

$$R\frac{\partial T/\partial t}{T} = D\frac{\partial^2 Z/\partial z^2}{Z} - U\frac{\partial Z/\partial z}{Z} = -\mu^2 \tag{12}$$

Solving the left member of Eq. (12) yields:

$$T = \alpha e^{-(\mu^2/R)t} \tag{13}$$

Likewise, solving the right member of Eq. (12) and taking into consideration that as the groundwater velocity U approaches zero, the discrimination becomes negative, that is, $U^2 - 4D\mu^2 < 0$ and hence complex conjugates result in this regard. The complementary solution corresponding to the complex roots $\frac{U}{2D} \pm \sqrt{-\frac{\mu^2}{D}}$ or $\frac{U}{2D} \pm \frac{\mu}{\sqrt{D}}i$ will be:

$$Z = e^{\frac{U}{2D}Z}\left(\beta\cos\frac{\mu}{\sqrt{D}}z + \gamma\sin\frac{\mu}{\sqrt{D}}z\right) \tag{14}$$

Substituting Eqs. (13) and (14) into Eq. (10):

$$\Phi(z,t) = e^{-(\mu^2/R)t}e^{\frac{U}{2D}z}\left(A\cos\frac{\mu}{D}z + B\sin\frac{\mu}{\sqrt{D}}z\right) \tag{15}$$

The arbitrary constants A and B can be determined via applying the new homogeneous boundary conditions at which $A = 0$. For n harmonics, Eq. (15) reduces to:

$$\Phi(z,t) = Be^{-(\mu^2/R)t}e^{\frac{U}{2D}z}\sin\frac{\mu}{\sqrt{D}}z \tag{16}$$

The B in Eq. (16) is determined by the Fourier half-range expansion:

$$\Phi(z,t) = \sum_{n=1}^{\infty} B_n e^{-\left(\frac{\mu_n^2}{R}\right)t}e^{\frac{U}{2D}z}\sin\frac{\mu_n}{\sqrt{D}}z \tag{17}$$

where:

$$\mu_n = \frac{n\pi}{\frac{H}{\sqrt{D}} + \frac{2\sqrt{D}}{U}} \tag{18}$$

$$B_n = \frac{2}{H}\int_0^H -C_o e^{\frac{U}{2D}z}\sin\frac{n\pi}{\frac{H}{\sqrt{D}} + \frac{2\sqrt{D}}{U}}z\,dz \tag{19}$$

$$C(z,t) = C_o + \sum_{n=1}^{\infty} B_n e^{-\left(\frac{\mu_n^2}{R}\right)t}e^{\frac{U}{2D}z}\sin\frac{\mu_n}{\sqrt{D}}z \tag{20}$$

Eq. (20) can only be applied for very low water velocity as in the flow of groundwater; furthermore, the substitution of this equation into the one-dimensional advection-dispersion [Eq. (1)] would not be satisfied unless the water velocity approaches zero.

4. Results and discussion

4.1. Description of reactive materials

Table 1 exhibits the physico-chemical properties for ZVI and ZVAI. Their appearance can be explained in Fig. 1 which signified the surface morphologies for ZVI and ZVAI at magnification powers of 100 μm for ZVI and 200 μm for ZVAI. The scanning electron microscopy (SEM) test was conducted using a scanner type FEI-S50, Japan. Fig. 1a exhibits the surface of the ZVI which is craggy by its nature to capture contaminants. Similarly, Fig. 1b exhibits the surface of the ZVAI which is characterized by large holes and cavities to entrap contaminants.

4.2. Longitudinal dispersion coefficient

The experimentally measured values of the hydrodynamic longitudinal dispersion coefficients using tracer experiments for the ZVI, ZVAI, and ZVI/ZVAI mixture are summarized in Table 2. This table exhibited different interstitial velocities (mean pore water velocities) which are somewhat analogous to the groundwater flow velocity since they satisfied the laminar flow pattern with Reynolds' number which is less than 10 [26].

The variation in simulated contaminated water velocity has produced a linear relationship relating the hydrodynamic longitudinal dispersion coefficient to the interstitial velocity. This relationship revealed that the dispersion coefficient is directly proportional to the pore water velocity and the hydrodynamic longitudinal dispersivity (α_L) and equals the slope of the line while the intercept of the dispersion axis was used to determine the effective molecular diffusion coefficient (Table 2). The hydrodynamic longitudinal dispersion coefficient was in the order of:

- (5–10) times greater than that of the effective molecular diffusion coefficient (≈10 cm^2/min for ZVI medium.
- (2–3) times greater than that of the effective molecular diffusion coefficient (≈35 cm^2/min for ZVAI medium.
- (3–5) times greater than that of the effective molecular diffusion coefficient (≈23 cm^2/min for ZVI/ZVAI medium.

Generally, the molecular diffusion coefficient for the media proposed in this study was almost lower than the hydrodynamic dispersion coefficients as in the ZVAI and ZVI/ZVAI media; or much lower than the hydrodynamic dispersion coefficient as in the ZVI medium. The reason for this variation can be elucidated that as narrowing the diameter of the columns in the present study, a negligible radial velocity and higher longitudinal velocity would result in this regard, that is, the transverse velocity has had little effect on the transverse hydrodynamic dispersion coefficient and thus generating low coefficient values.

4.3. One-dimensional model development

The advection–dispersion partial differential equation is used to describe the equilibrium contaminant transport through the PRB taking the sorption process into account. This equation was solved analytically as described previously with the application of the boundary conditions (at the boundaries of the proposed column) and the initial condition at the same distance along the column (distance between successive ports) and for adequate time intervals. The basic configuration of the columns system was made up of five columns, 125 cm by 1.6 cm in diameter each, the diameter was intentionally chosen as 1.6 cm for the following reasons:

- The apparent cross-sectional area of the column would equal to 2 cm^2 and this would facilitate the interstitial water velocities calculations since the actual pore water flow area becomes 1 cm^2 corresponding to nearly 0.5 porosity and as a result; the magnitude of the interstitial water velocity would be as the same as that of the water flow rate.
- The narrowing of the column diameter would bring about one-dimensional upward water flow with neglecting radial water flow velocities and their corresponding transverse hydrodynamic dispersion coefficients.

The contaminated solution with a concentration of 50 mg/L was fed to the packed columns from the bottom base. The reason for installing five columns with different sorbent depths has had two folds' objectives; the first is to take average values for the effluent concentrations and the second is to provide extra time and take the opportunity for other concentration measurements without the frequent need for the sorbent regeneration. The necessary constants and parameters for the PRB bed utilized in the one-dimensional solute transport model can be explained in Table 3.

4.4. Measured breakthrough of Cd(II)/Cr(III) in the ZVI and ZVAI bed

Breakthrough curves have been obtained by normalizing the contaminant concentration from the results

Table 1
Physico-chemical properties for ZVI and ZVAI

Property	Value	
	ZVI	ZVAI
Solid density (g/cm^3)	7.87	2.70
Bulk density (g/cm^3)	4.175	1.350
Iron (%)	90	–
Aluminum (%)	–	94
Specific surface area (m^2/g)	0.67	7.8
Atomic number	26	13
Atomic mass	56	27
Melting point (°C)	1,537	627
Boiling point (°C)	2,861	660

Table 2
Experimental hydrodynamic longitudinal dispersion coefficients for ZVI and ZVAI PRB medium as a function of interstitial velocity

Medium and parameter		Flow rate (mL/min)			
		3	4.5	6	7.5
ZVI	U (cm/min)	3.19	4.78	6.38	7.97
	D_L (cm^2/min)	54	76	98	120
	α_L (cm)	14.66			
ZVAI	U (cm/min)	3	4.5	6	7.5
	D_L (cm^2/min)	60	74	85	98
	α_L (cm)	8.33			
ZVI + ZVAI	U (cm/min)	2.9	4.5	5.9	7.5
	D_L (cm^2/min)	58	78	95	112
	α_L (cm)	11.93			

already obtained from the experimental values. The experimental breakthrough curves for each metal uptake corresponding to flow rates of 3 and 4.5 mL/min for different intervals and locations along each column packed with different sorbents are shown in Fig. 3. This figure in conjunction with Table 3 revealed that as the contaminant velocity increases, the probability for the contaminant to be captured on the sorbent medium decreases; therefore, the distribution coefficient and the retardation factor also decrease. This renders the contaminants to emerge faster and as a consequence; the breakthrough curves would be steeper S-shaped and extended upward in contrast with the lower velocities that guarantees the partitioning of the contaminants over the solid medium which increases both the distribution coefficient and the retardation factor that hinders the movement of the contaminant flow and diminishes the probability of the contaminant emergence.

Table 3
Constants and parameters utilized for the cadmium and chromium transport in one-dimensional column model

Parameter	Value		
	ZVI	ZVAI	ZVAI + ZVI
Depth (m)	0.2–1		
Porosity	0.5		
Bulk density (g/cm^3)	4.175	1.350	3.570
α_L (cm)	14.66	8.33	11.93
Interstitial velocity (U, cm/min)	3 and 4.5		
Distribution coefficient (k_d, L/g)	0.0022–0.0055		
Retardation factor (R)	13.7–20.5		
Initial condition (C(z,0), mg/L)	Zero		
Boundary conditions	50 mg/L @ inlet of bed, advective flux at end of bed		

When the velocity had increased from 3 to 4.5 cm/min; the distribution coefficient decreased consequently from 0.0022 to 0.0017 L/g, that is, 23% a decrease in the k_d for the sorption of a single Cr(III) onto ZVI that made the retardation factor to be reduced from 20.5 to 15.2, that is, 26% a decrease. Although the distribution coefficient for the chromium ions onto ZVI is less than that in cadmium ions onto ZVAI by 60%, the bulk density for the ZVAI is less than that of ZVI by 68% which makes the retardation to the chromium ions more than that in cadmium ones. Therefore, the shape of the breakthrough curves for the Cr(III) is broader than that in Cd(II) at the same interstitial velocity and bed depth. Also, when the velocity had increased from 3 to 4.5 cm/min; the distribution coefficient decreased from 0.0055 to 0.0047 L/g, that is, 15% a decrease in the k_d for the sorption of Cd(II) onto ZVAI that made the retardation factor to be reduced from 16 to 13.7, that is, 14% a decrease.

The breakthrough curves for the sorption of cadmium or chromium ions onto the ZVI/ZVAI composite sorbent (Fig. 4) reveals that, for instance, at depth 100 cm and interstitial water velocity 3 cm/min, the concentrations for cadmium ions were 34 and 46 mg/L while for chromium ions were 23 and 40 mg/L after time laps of 12 and 24 h respectively. This elucidates that the chromium ions have relatively more affinity to and highly hindered by the mixture ZVI/ZVAI; therefore, chromium emerged slower than

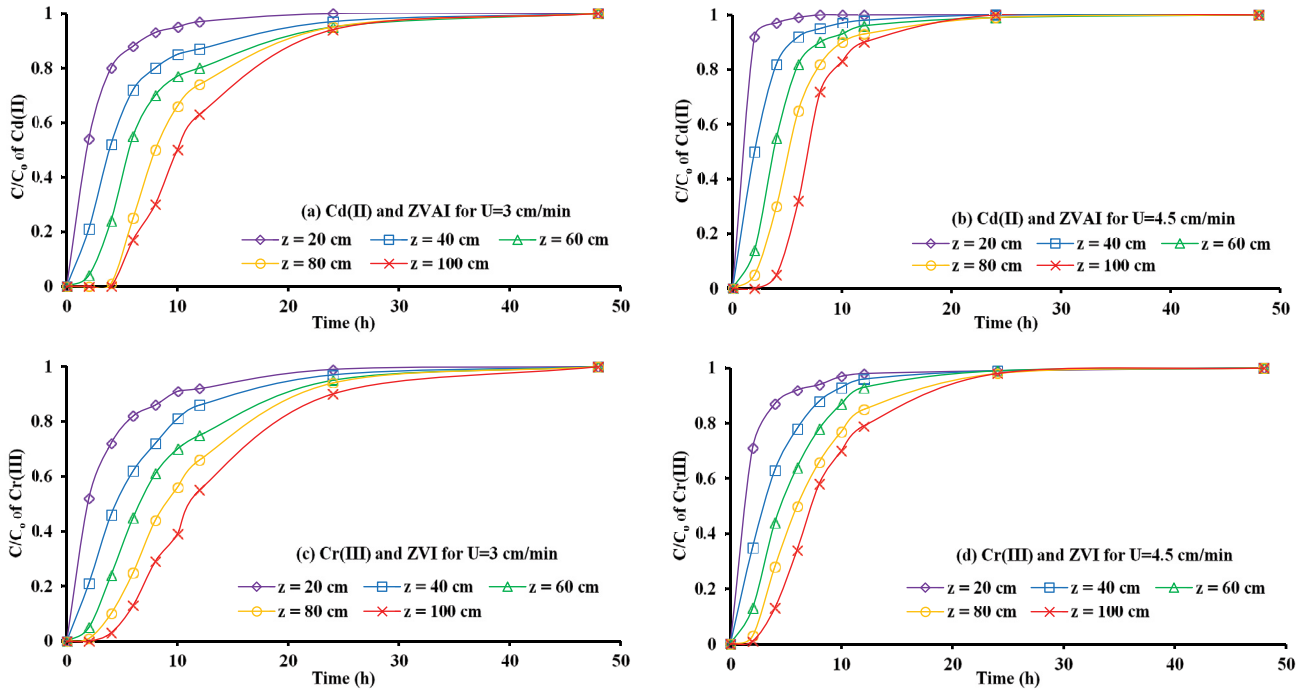

Fig. 3. Experimental breakthrough curves for Cd(II) and Cr(III) uptake by ZVAI and ZVI respectively at different values of interstitial.

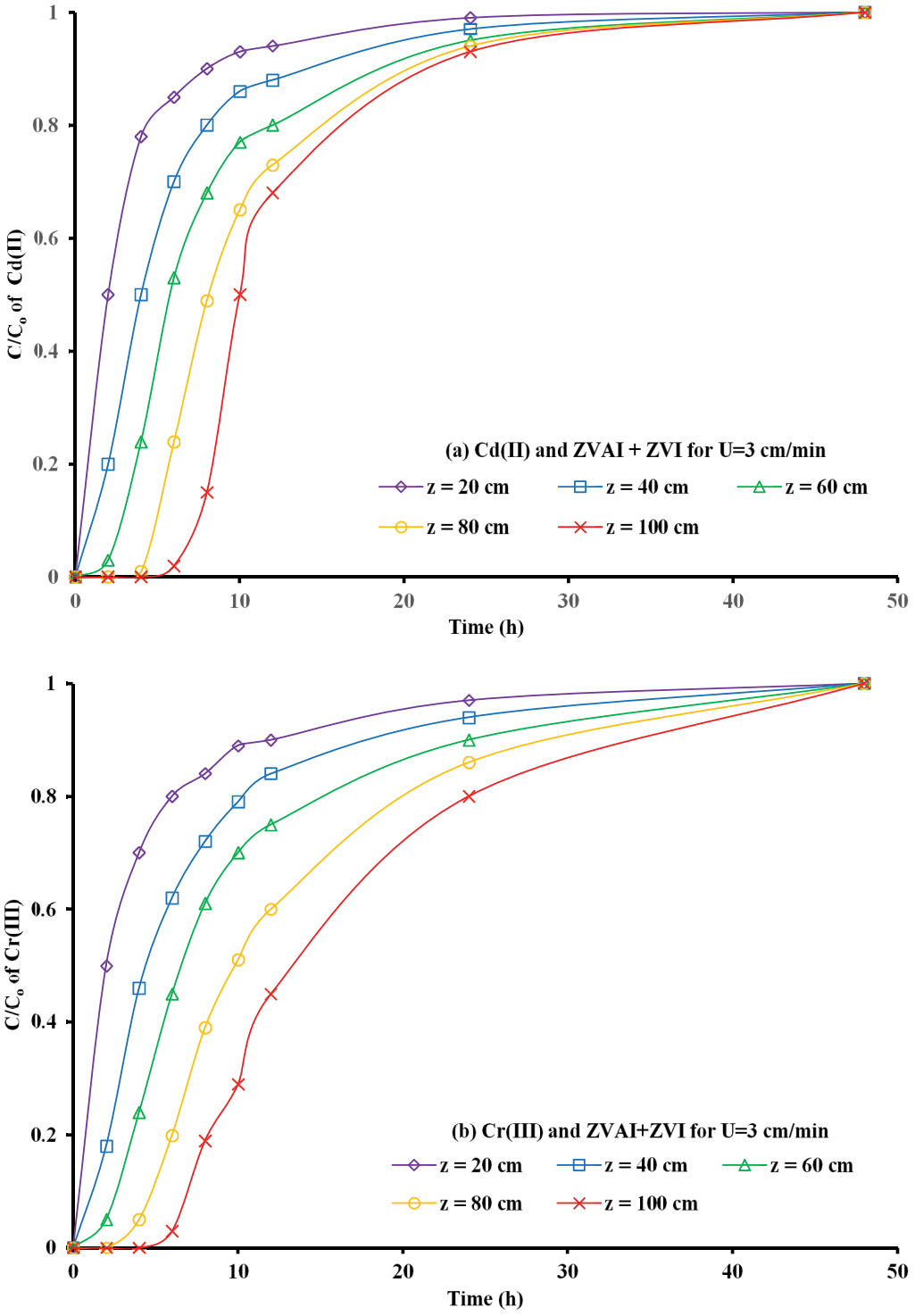

Fig. 4. Experimental breakthrough curves for Cd(II) and Cr(III) uptake by ZVAI/ZVI composite sorbent at interstitial velocity equal to 3 cm/min.

cadmium and this is obvious from the orientation, direction, and shape of the breakthrough curves. Previous researches like [27] have demonstrated that ZVI or ZVAI alone as the reactive medium had some limitations in removing contaminants from water. Despite the amenability of ZVI to oxidation by the presence of oxygen in wastes, the mixing up of ZVI with ZVAI inappropriate mass proportions will enhance the effectiveness of the removal process since the standard reduction potential for aluminum is (–1.67 V Al^{+3}/Al) which is much lower than that of iron (–0.44V Fe^{+2}/Fe);

therefore the aluminum is strong reducing agent while iron plays an important role in carrying off the electrons donated by aluminum; furthermore, aluminum can also reduce iron ions (Fe^{++} and Fe^{+++}) to prevent them to form iron corrosion products (iron oxides) on the ZVI surface and thereby maintain the surface activity of the ZVI [15].

4.5. Breakthrough modelling

Breakthrough curves have appreciable design outcomes in the column study at which concentration-time dependent data contribute to the revelation of the surface characteristics, affinity, and sorption phenomena for the sorbents [18,28]. The mathematical model derived (Sec.3) was applied to provide comparisons between the analytical (predicted) and experimental normalized concentrations for the contaminant(s) sorption onto each sorbent material(s). Fig. 5 shows comparisons between analytical and experimental normalized concentrations for the sorption of Cd(II) and Cr(III) onto ZVAI and ZVI and at different water interstitial velocities, this figure revealed a good agreement between the analytical and experimental results. This could be attributed to taking the sorption onto the bed, that is, retardation factor of the contaminant on the sorbent is greater than 1 in the present model.

To make informative evaluations on the accuracy of the outcome, predicted values were compared to the measured ones in a meaningful quantitative way. The coefficient of determination R^2 alone is not precise indicative for the data analysis; therefore, a powerful statistical measure of Nash–Sutcliff [29] was introduced to determine the degree of perfectness between the analytical (expected) and the experimental (observed) values at which 1 is assigned to perfect agreement. In the present study, the Nash–Sutcliff efficiency was found to be greater than 0.98 and this is an indication that the derived mathematical model is more representative based on the experimental and predicted results adopted.

4.6. Measured breakthrough of Cd(II) and Cr(III) binary system through ZVAI + ZVI composite bed

For the interaction of the binary system with a composite sorbent bed, Fig. 6a and b, signified that the experimental breakthrough curves have relatively skewed to the right and broader than that of Fig. 3. This elucidated the sort of competition induced among contaminant species Cr(III) and Cd(II) for the sorption onto the active sites available, also they possess a relatively high distribution coefficient that increases their retardation factor, a comparison can be shown in Fig. 6c; therefore, retention and delay for the emergence of these contaminants occurred corresponding to a wider or broader extension for the breakthrough curves to the right.

In practice, the magnitude of the groundwater velocity is much less than that proposed in the experiments conducted; therefore, two additional contaminant interstitial velocities of 0.25 and 0.5 cm/min corresponding to flow rates of 0.25 and 0.5 mL/min for the binary chromium metal uptake column study were examined respectively. It was found that from Fig. 6d, each breakthrough curves up to 168 h have had no definite exhaustion points (time required for the normalized concentration C/C_o to reach 1), but they have had breakthrough points (time required for the

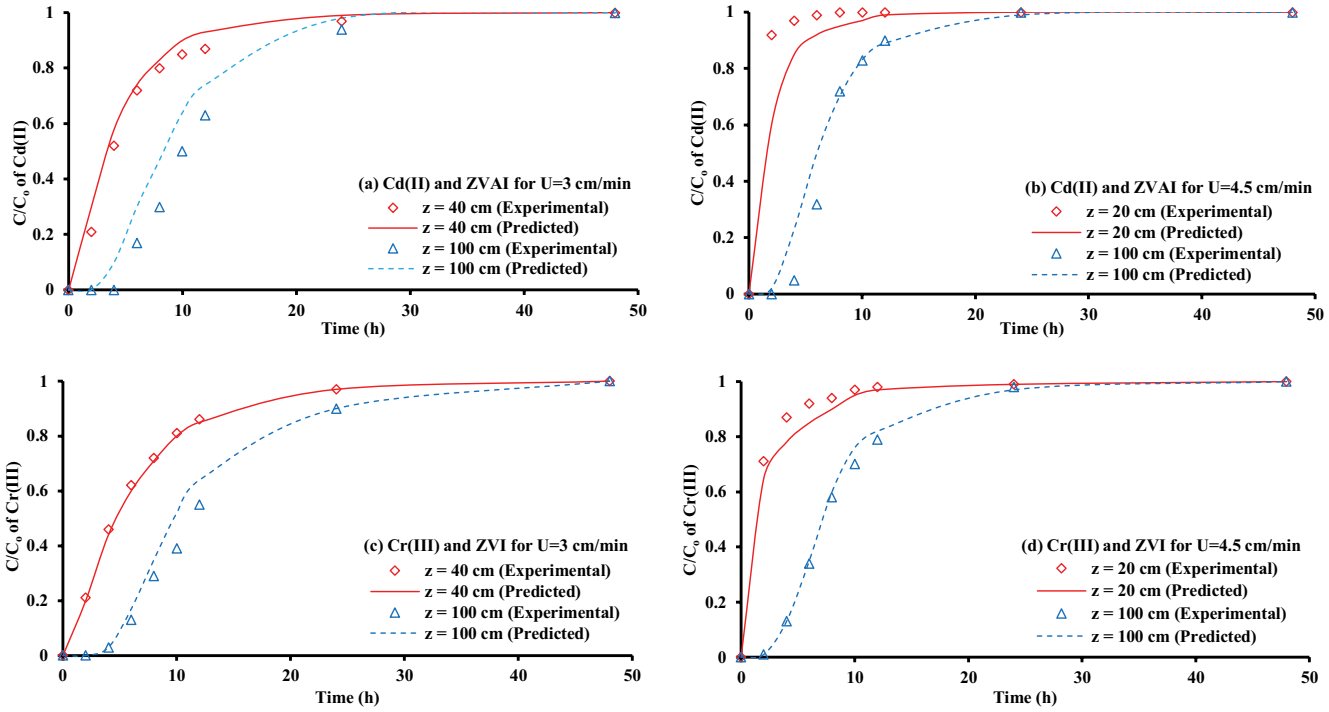

Fig. 5. Comparison between analytical solution and experimental results of Cd(II) and Cr(III) concentrations in the column packed with ZVAI and ZVI beds respectively for different values of interstitial velocity.

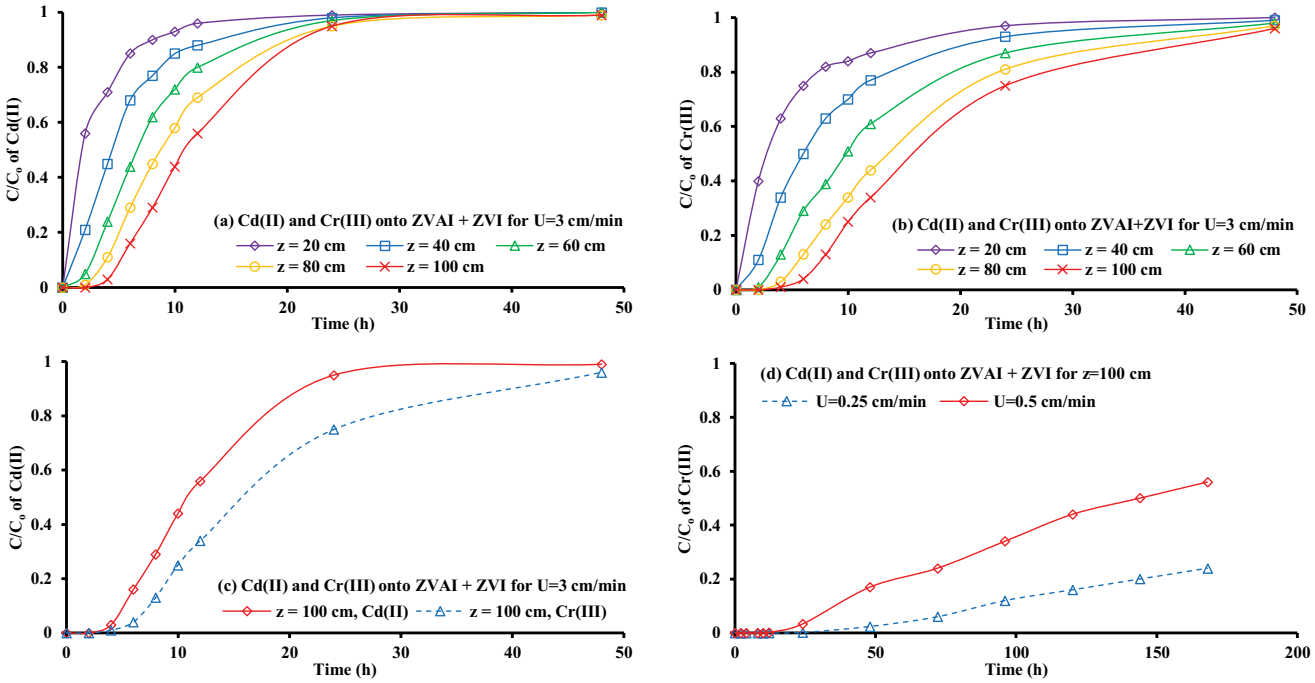

Fig. 6. Experimental breakthrough curves for binary metals (cadmium and chromium) uptake by composite sorbent at different locations and interstitial velocities.

normalized concentration C/C_o to reach 0.05 or 0.1) of 72 h and 48 h for the binary chromium metal uptake corresponding to contaminant interstitial velocities of 0.25 and 0.5 cm/min respectively. The curve corresponding to pore water velocity of 0.5 cm/min is more extended upward than that with 0.25 cm/min; this is due to the early emergence of the contaminant. The exhaustion point can determine the time required for regenerating the remediation barrier; the proposed low water velocities, particularly the 0.25 cm/min is more representative for the groundwater flow velocity.

4.7. Barrier longevity

The collected volumes of the treated water from the packed column in the present study were assumed as adequate as that flowing in the vicinity of soil where the ZVAI + ZVI sorbent is placed; furthermore, the hydraulic conductivity (K) of the reactive barrier must be equal or greater than that of the soil; the value of K may be assigned to 1.01×10^{-5} m/s that is similar to the value of the sandy soil while the hydraulic gradient values for the groundwater flow in the flat plane lands may be taken within the range (0.001–0.01) m/m [23]. Based upon the permissible contaminant concentrations for cadmium and chromium mentioned previously (Sec.1), the longevity of the PRB using the upper bound of the hydraulic gradient range was estimated to be 210 and 250 d to produce cadmium and chromium effluent ions respectively beyond 100 cm barrier matrix within these permissible concentrations. However, the interstitial water velocities of the contaminants were relatively higher than the actual groundwater velocity; therefore, another run for a continuous study was re-conducted under the same conditions and simulate the real status of the groundwater velocity. Velocities of 0.25 and 0.5 cm/min were proposed for the binary chromium uptake (Fig. 6d); it was found that the corresponding longevity was calculated to be 7.02 y for the capture of chromium ions onto the composite mixture of ZVI/ZVAI; this elucidated that the lower contaminant velocity, the more longevity barrier is satisfied to meet the standard limits for the permissible contaminant concentration.

5. Conclusions

The results of the column study proved that the lower the metal ions velocity, the higher the distribution coefficient and high retardation for these ions (the retardation depends mainly on the physical characteristics of the sorbate such as distribution coefficient of the contaminant over the solid medium and velocity of the contaminant as well as the physical characteristics of the sorbent such as bulk density and porosity) is resulted which made the breakthrough curves broader and extended to the right rather than being steep and extended upward. For the breakthrough curves, the predictions of the developed mathematical model solved analytically by separation of variables are in good concurrence with experimental measurements where Nash–Sutcliff efficiency is greater than 0.98. Also, the normalized concentrations in the binary system were relatively lower than those for single systems; this is due to the competition among contaminants in the binary mode. The SEM images for the ZVI and ZVAI before interaction with the metal ions revealed that the surfaces of these sorbents contain cavities, groovy lumps, rough and smooth texture, open, and closed pore channels. Finally, the longevity of the PRB based on maximum hydraulic conductivity equivalent to 1.01×10^{-5} m/s (critical status) and

the upper bound of the hydraulic gradient 0.01 m/m was found to inversely proportional to the contaminant velocity. This means that the longevity of the barrier is increased with the lower velocity that brought about high retardation to the plume propagation and consequently makes the contaminant reach its permissible concentration after a longer time.

Acknowledgements

One of the authors (B. Saleh) is grateful to the Taif University Researchers Supporting Project number (TURSP-2020/49), Taif University, Taif, Saudi Arabia for the financial support. Also, the authors would like to gratefully acknowledge the technical support of Environmental Engineering Department/ University of Baghdad during this work.

References

[1] R. Awual, G.E. Eldesoky, T. Yaita, Mu. Naushad, H. Shiwaku, Z.A. Alothman, S. Suzuki, Schiff based ligand containing nanocomposite adsorbent for optical copper(II) ions removal from aqueous solutions, Chem. Eng. J., 279 (2015) 639–647.
[2] A.H. Sulaymon, A.A.H. Faisal, Z.T. Abd Ali, Performance of granular dead anaerobic sludge as permeable reactive barrier for containment of lead from contaminated groundwater, Desal. Water Treat., 56 (2015) 327–337.
[3] S.S. Alquzweeni, A.A.H. Faisal, Possibility of using granular iron slag byproduct as permeable reactive barrier for remediation of simulated water contaminated with lead ions, Desal. Water Treat., 178 (2020) 211–219.
[4] R. Tog, G. Zeitsmann, B. Tena, Presence of heavy metals in water environment, fate and impacts, J. Hazard. Mater., 53 (2007) 56–87.
[5] A.A.H. Faisal, M.M. Ibreesam, N. Al-Ansari, L. Naji, M. Naushad, T. Ahamad, COMSOL multiphysics 35a package for simulating the cadmium transport in the sand bed-bentonite low permeable barrier, J. King Saud Univ. - Sci., 32 (2020) 1944–1952.
[6] M. Hashim, S. Mukhopadhyay, J. Sahu, B. Sengupta, Remediation technologies for heavy metal contaminated groundwater, J. Environ. Manage., 92 (2011) 2355–2388.
[7] C.C. Travis, C.B. Doty, Can contaminated aquifers at superfund sites be remediated?, Environ. Sci. Technol., 24 (1990) 1464–1466.
[8] A.A.H. Faisal, A.H. Sulaymon, Q.M. Khaliefa, A review of permeable reactive barrier as passive sustainable technology for groundwater remediation, Int. J. Environ. Sci. Technol., 15 (2018) 1123–1138.
[9] G. Bartzas, K. Komnitsas, Solid phase studies and geochemical modelling of low-cost permeable reactive barriers, J. Hazard. Mater., 183 (2010) 301–308.
[10] M. Chang, K. Wang, R. Chin, Transport modeling of copper and cadmium with linear and nonlinear retardation factors, Chemosphere, 43 (2001) 1133–1139.
[11] H.L. Lien, R.T. Wilkin, High-level arsenite removal from groundwater by zero-valent iron, Chemosphere, 59 (2005) 377–386.
[12] J.R. Gonzalez, J.C. Walton, Modeling the adsorption of Cr(III) from aqueous solution onto *Agave lechuguilla* biomass, study of the advective and dispersive transport, J. Hazard. Mater., 15 (2009) 234–512.
[13] F. Fu, D. Dionysiou, H. Liu, The use of zero-valent iron for groundwater remediation and wastewater treatment: a review, J. Hazard. Mater., 267 (2014) 194–205.
[14] A.A.H. Faisal, T.R. Abbas, S.H. Jassam, Removal of zinc from contaminated groundwater by zero-valent iron permeable reactive barrier, Desal. Water Treat., 55 (2015) 1586–1597.
[15] W. Han, F. Fu, Z. Cheng, B. Tang, S. Wu, Studies on the optimum conditions using acid washed zero-valent iron/zero-valent aluminum mixtures in permeable reactive barriers for the removal of different heavy metal ions from wastewater, J. Hazard. Mater., 302 (2016) 437–446.
[16] A.A.H. Faisal, Z.A. Hmood, Groundwater protection from cadmium contamination by zeolite permeable reactive barrier, Desal. Water Treat., 53 (2015) 1–10.
[17] A.A.H. Faisal, M.D. Ahmed, Removal of copper ions from contaminated groundwater using waste foundry sand as permeable reactive barrier, Int. J. Environ. Sci. Technol., 12 (2015) 2613–2622.
[18] A.H. Sulaymon, A.A.H. Faisal, Q.M. Khaliefa, Cement kiln dust (CKD)-filter sand permeable reactive barrier for the removal of Cu(II) and Zn(II) from simulated acidic groundwater, J. Hazard. Mater., 297 (2015) 160–172.
[19] A.A.H. Faisal, Z.T. Abd Ali, Groundwater protection from lead contamination using granular dead anaerobic sludge biosorbent as permeable reactive barrier, Desal. Water Treat., 57 (2016) 3891–3903.
[20] A.A.H. Faisal, S.F.A. Al-Wakel, H.A. Assi, L.A. Naji, M. Naushad, Waterworks sludge-filter sand permeable reactive barrier for removal of toxic lead ions from contaminated groundwater, J. Water Process Eng., 33 (2020) 101112, doi: 10.1016/j.jwpe.2019.101112.
[21] M. Abdul-Kareem, A. Faisal, Removal of copper and cadmium ions from contaminated groundwater by iron oxide/hydroxide-coated sand in the permeable reactive barrier technology, Desal. Water Treat., 182 (2020) 208–219.
[22] L.A. Naji, A.A.H. Faisal, H.M. Rashid, Mu. Naushad, T. Ahamad, Environmental remediation of synthetic leachate produced from sanitary landfills using low-cost composite sorbent, Environ. Technol. Innov., 18 (2020) 100680, doi: 10.1016/j.eti.2020.100680.
[23] J. Bear, A.H.-D. Cheng, Modeling Groundwater Flow and Contaminant Transport, Springer Netherlands, Dordrecht, 2010.
[24] A. Kumar, D.K. Jaiswal, N. Kumar, Analytical solutions of one-dimensional advection-diffusion equation with variable coefficients in a finite domain, J. Earth Syst. Sci., 118 (2009) 539–549.
[25] A. Kumar, D.K. Jaiswal, R.R. Yadav, Analytical solutions of one-dimensional temporally dependent advection-diffusion equation along longitudinal semi-infinite homogeneous porous domain for uniform flow, IOSR J. Math., 2 (2012) 1–11.
[26] A.A.H. Faisal, Z.T. Abd Ali, Using granular dead anaerobic sludge as permeable reactive barrier for remediation of groundwater contaminated with phenol, J. Environ. Eng., 141 (2015) 04014072.
[27] L. Liang, N. Korte, B. Gu, R. Puls, C. Reeter, Geochemical and microbial reactions affecting the long-term performance of in situ 'iron barriers,' Adv. Environ. Res., 4 (2000) 273–286.
[28] J. Goel, K. Kadirvelu, C. Rajagopal, V. Kumar Garg, Removal of lead(II) by adsorption using treated granular activated carbon: batch and column studies, J. Hazard. Mater., 125 (2005) 211–220.
[29] P. Krause, D.P. Boyle, F. Bäse, Comparison of different efficiency criteria for hydrological model assessment, Adv. Geosci., 5 (2005) 89–97.